

# Development of Lipidoid–siRNA Formulations for Systemic Delivery to the Liver

Akin Akinc<sup>1</sup>, Michael Goldberg<sup>2</sup>, June Qin<sup>1</sup>, J Robert Dorkin<sup>1</sup>, Christina Gamba-Vitalo<sup>1</sup>, Martin Maier<sup>1</sup>, K Narayanannair Jayaprakash<sup>1</sup>, Muthusamy Jayaraman<sup>1</sup>, Kallanthottathil G Rajeev<sup>1</sup>, Muthiah Manoharan<sup>1</sup>, Victor Koteliansky<sup>1</sup>, Ingo Röhl<sup>3</sup>, Elizaveta S Leshchiner<sup>4</sup>, Robert Langer<sup>4</sup> and Daniel G Anderson<sup>4</sup>

<sup>1</sup>Alnylam Pharmaceuticals, Inc., Cambridge, Massachusetts, USA; <sup>2</sup>Department of Chemistry, Massachusetts Institute of Technology, Cambridge, Massachusetts, USA; <sup>3</sup>Roche Kulmbach GmbH, Kulmbach, Germany; <sup>4</sup>David H. Koch Institute of Integrative Cancer Research, Massachusetts Institute of Technology, Cambridge, Massachusetts, USA

RNA interference therapeutics afford the potential to silence target gene expression specifically, thereby blocking production of disease-causing proteins. The development of safe and effective systemic small interfering RNA (siRNA) delivery systems is of central importance to the therapeutic application of siRNA. Lipid and lipid-like materials are currently the most well-studied siRNA delivery systems for liver delivery, having been utilized in several animal models, including nonhuman primates. Here, we describe the development of a multicomponent, systemic siRNA delivery system, based on the novel lipid-like material 98N<sub>12</sub>-5(1). We show that *in vivo* delivery efficacy is affected by many parameters, including the formulation composition, nature of particle PEGylation, degree of drug loading, and biophysical parameters such as particle size. In particular, small changes in the anchor chain length of poly(ethylene glycol) (PEG) lipids can result in significant effects on *in vivo* efficacy. The lead formulation developed is liver targeted (>90% injected dose distributes to liver) and can induce fully reversible, long-duration gene silencing without loss of activity following repeat administration.

Received 5 December 2008; accepted 6 February 2009; published online 3 March 2009. doi:10.1038/mt.2009.36

## INTRODUCTION

RNA interference offers a powerful platform for functional genomics, *in vivo* target validation, and gene-specific medicines.<sup>1</sup> Unlike small molecules, which are generally limited to binding to and blocking ion channels, receptors, and enzymes, small interfering RNAs (siRNAs) may be used to modulate the expression of nearly any gene transcript—endogenous or exogenous—in a specific manner.<sup>2</sup> The emergence of genetic therapies may enable physicians to replace defective genes and to modulate their expression specifically.<sup>3</sup> A key to the therapeutic application of RNA interference is the advancement of efficient and safe nucleic acid delivery *in vivo*.<sup>4</sup> Because virus-mediated delivery

is associated with safety concerns,<sup>5,6</sup> nonviral nucleic acid delivery has attracted a great deal of interest.<sup>7</sup> In addition to chemical modification of naked nucleic acids,<sup>8</sup> synthetic vectors have been created to improve biostability<sup>9</sup> and to facilitate delivery. Polycationic lipids can electrostatically bind and condense nucleic acids to form nanometer-sized complexes,<sup>10</sup> enabling enhanced cellular uptake.<sup>11</sup>

Several delivery systems for systemic siRNA delivery have been recently described.<sup>2,12–23</sup> Of all the carriers, cationic, lipid-based formulations are currently the most widely validated means for systemic delivery of siRNA to the liver.<sup>24</sup> The liver is an important organ with a number of potential therapeutic siRNA targets—including cholesterol biosynthesis, fibrosis, hepatitis, and hepatocellular carcinoma—whose parenchymal cells are accessible through fenestrated endothelium (100–150 nm).<sup>25</sup>

In general, lipid-based nanoparticles are thought to enter cells by endocytosis,<sup>26,27</sup> and it has been hypothesized that certain cationic lipids can mediate endosomal escape by destabilizing the endosomal membrane<sup>28</sup> or by causing endosomal rupture via the “proton sponge” mechanism.<sup>29</sup> Excessive charge is, however, associated with certain negative consequences *in vivo*, including non-specific interactions with biological surfaces, increased protein binding, opsonization, rapid clearance by the reticuloendothelial system, hemolysis, and cytotoxicity.<sup>30</sup>

The synthesis and screening of a novel combinatorial cationic lipidoid library has led to the identification of a number of effective novel, systemic siRNA delivery vehicles.<sup>31</sup> The library was generated by the conjugated addition of primary or secondary amines to alkyl-acrylates or alkyl-acrylamides. *In vitro* activity of the lipidoids was demonstrated in multiple cell types, and *in vivo* efficacy was demonstrated against multiple gene targets in multiple animal species, including nonhuman primates. In this study, we extended our prior work by investigating the impact of various formulation parameters on *in vivo* pharmacodynamics. *In vivo* efficacy of the lipidoid–siRNA formulations were evaluated using a mouse hepatic gene silencing model, and tolerability was assessed by observation of animals at the cage side and by monitoring of animal body weights. We used this data to develop a lipidoid-based

**Correspondence:** Akin Akinc, Alnylam Pharmaceuticals, Inc., 300 Third Street, Cambridge, Massachusetts 02142, USA. E-mail: [aakinc@alnylam.com](mailto:aakinc@alnylam.com) or Daniel G Anderson, David H. Koch Institute of Integrative Cancer Research, Massachusetts Institute of Technology, 45 Carleton Street, Building E25-342, Cambridge, Massachusetts 02142, USA. E-mail: [dgander@mit.edu](mailto:dgander@mit.edu)

formulation for the delivery of systemically administered siRNA to liver. Specific parameters that we investigated included formulation composition, nature of particle PEGylation, degree of siRNA loading, and particle size. We then investigated key attributes—biophysical characteristics, formulation stability, pharmacokinetics, biodistribution, and ability to maintain activity upon repeat administration—of the optimized formulation to assess pharmaceutical suitability of the formulation.

## RESULTS

### Preliminary formulation design

Liposomes and lipid-based formulations have been used clinically to enhance the pharmacokinetic and pharmacodynamic properties of drugs.<sup>32,33</sup> Ideally, formulation of drug in lipids results in the specific delivery of the drug to the target tissue, which in our case was liver parenchyma. However, cationic lipid formulations often accumulate in lungs and spleen, in addition to liver.<sup>34</sup> Furthermore, in many cases, it is the reticuloendothelial system (Kupffer cells) of the liver and not the parenchyma (hepatocytes) that take up the majority of the liver-associated material. Other considerations specific to nucleic acid delivery include protection against nuclease degradation in the blood and the requirement of intracellular delivery for activity. With these principles in mind, we developed a lipidoid-based formulation for the delivery of siRNA to hepatocytes *in vivo*.

The three-component delivery system was based on the novel lipidoid 98N<sub>12</sub>-5(1) and also included cholesterol and the poly(ethylene glycol) (PEG) lipid mPEG<sub>2000</sub>-C14 glyceride (Figure 1). We selected these additional excipients as they have a history of use in the formation of stable nanoscale lipid particles.<sup>15,34–37</sup> Cholesterol is found naturally in lipid membranes and can provide structure to bilayers by occupying the space between lipid tails. PEGylation, in the form of a PEG lipid inserted into the lipid particles, helps to prevent aggregation and promotes the stability of nanometer-sized particles, as well as facilitating increased circulation time. As our goal was to achieve delivery to hepatocytes accessible via 100–150-nm-sized endothelial fenestrae, inclusion of a PEG lipid in the formulation was critical to the formation of small, nonaggregated particles. With typical literature values for molar ratios of cholesterol (30–50%) and PEG lipid (5–10%) as a starting point, we optimized the lipid composition to

achieve a robust formulation with good *in vivo* activity. The final lipid composition was 98N<sub>12</sub>-5(1):cholesterol:PEG-lipid = 42:48:10 (mol:mol:mol).

### Maximizing siRNA loading

We hypothesized that siRNA loading would be an important parameter affecting the *in vivo* activity of lipidoid-siRNA formulations. For a given dose of siRNA, a higher siRNA loading results in a lower dose of administered lipid. Decreasing the dose of lipid *in vivo* could decrease toxicity; however, it could also decrease efficacy. Efficacy may be impaired as a result of reduced charge on the particles, which could decrease cellular uptake, or by reducing the ability of the particles to destabilize cellular membranes. The balance between efficacy and toxicity is not uncommon with lipid-based transfection reagents. We first sought to determine the maximal loading ratio by progressively decreasing the initial lipid (98N<sub>12</sub>-5(1), cholesterol, and PEG lipid):siRNA weight ratio and measuring the resultant percent entrapment of the siRNA in the final formulation (Figure 2a). Entrapment of siRNA was determined using the Quant-iT RiboGreen RNA assay. At higher initial lipid:siRNA ratios, the lipids are in excess such that siRNA binding capacity has not been reached and the final percent entrapment is >95%. When the initial lipid:siRNA ratio is decreased to the point where the siRNA is in excess and the binding capacity of the lipid nanoparticles has been saturated, the excess siRNA remains as free, untrapped siRNA, and the final percent entrapment of the formulation decreases. Using this approach, we determined that maximal siRNA loading occurs at a lipid:siRNA of ~7.5:1 (wt:wt). Furthermore, if desired, loading can be done at lower lipid:siRNA ratios, and the excess siRNA can be removed by tangential flow filtration using a 100,000 molecular weight cutoff membrane (Figure 2b).

To examine the impact of maximizing siRNA loading on *in vivo* efficacy and tolerability, we dosed mice at a constant siRNA dose of 1.5, 2, and 10 mg/kg using formulations of differing lipid:siRNA ratios. Consequently, animals dosed with formulations with higher lipid:siRNA ratios received higher doses of the lipid components. Animals were observed, body weights were recorded, and serum was collected for analysis of Factor VII gene silencing 2 days after administration. At the two lower doses, all formulations were well tolerated and normal weight gain was observed. However, at the

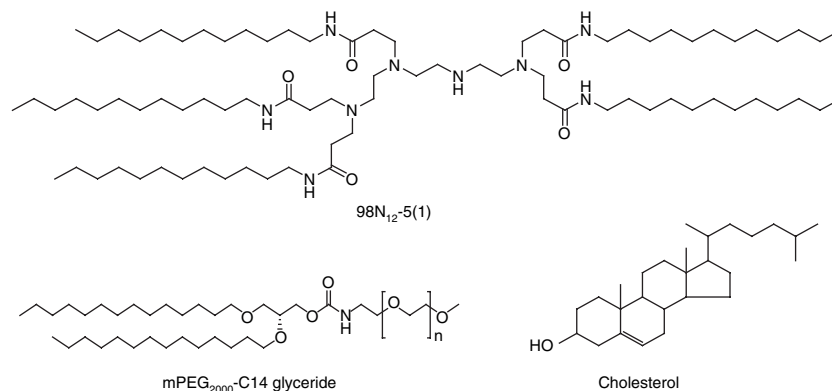


Figure 1 The structures of 98N<sub>12</sub>-5(1), the five-tailed isomer of triethylenetetramine-laurylaminopropionate with a free internal amine, Cholesterol, and mPEG<sub>2000</sub>-C14 Glyceride.

10 mg/kg dose, only the formulation with lipid:siRNA ratio of 7.5:1 was associated with normal weight gain. At the highest dose level we observed a dose-dependent trend in decreased tolerability as lipid:siRNA ratio increased from 7.5:1 to 30:1 as evidenced by a trend in weight loss and death of the animals in the 30:1 formulation group (Figure 2c). All formulations mediated effective silencing of Factor VII *in vivo*, with a slight trend in decreased efficacy as lipid:siRNA ratio is lowered (Figure 2d). Although we recognized the slight decrease in efficacy at lower lipid:siRNA ratios, we felt that the increase in tolerability outweighed this effect; thus, we confirmed our initial choice of using the minimum amount of lipid required to encapsulate siRNA and settled on a final lipid:siRNA ratio of 7.5:1 (wt:wt).

### PEG lipid alkyl chain length dramatically affects *in vivo* activity

PEG influences particle interaction with cells, biological matrices, and blood components, which in turn affect efficacy and toxicity.<sup>38</sup> The extent of particle PEGylation and the rates at which particles lose PEG shielding are known to have significant effects on formulation pharmacokinetics.<sup>39</sup> Because the lipid portion of the PEG-lipid conjugate enables PEG to be hydrophobically, rather than covalently, incorporated into the particles, the PEG exchange, and thus, deshielding rate, can be controlled by changing the hydrophobicity of the PEG lipid. This can be accomplished by varying the length of the alkyl chain lipid anchor.<sup>40</sup> Initially, we explored the use of lipid anchor lengths of 14, 16, and 18 carbons (C14, C16, and C18) and found that this parameter had a significant effect on *in vivo* activity, with the shortest anchor length resulting in the greatest efficacy. Therefore, we sought to determine the optimal length of the hydrophobic lipid tail. A glycerol backbone

was derivatized with one PEG chain (MW 2000) and two alkyl chains of various lengths, ranging from C10 to C16.

The PEG lipids were incorporated into the formulation, resulting in particles 50–60 nm in diameter in all cases, and activity was assessed at two dose levels, 2.5 and 20 mg/kg (Figure 3a,b). Formulations containing tail lengths of C13, C14, and C15 displayed similar activities, demonstrating superior efficacy to formulations with both shorter tail length, C10–C12, and longer tail length, C16. We also noted a general trend toward improved tolerability with increasing tail length. Overall, we found that C14- and C15-based PEG lipids yielded formulations with good activity. As the starting materials for synthesis of even-tailed PEG-lipids are more readily available than odd-tailed PEG-lipids, we selected the C14 lipid anchor length.

### Optimization of particle size

In order to access hepatocytes via the systemic circulation, material must pass through the fenestrations of the liver endothelium. The size of the fenestrae (100–150 nm), therefore, places a limit on the size of particles that can effectively access hepatocytes. We hypothesized that formulations with a smaller particle size distribution would more effectively deliver siRNA to hepatocytes and thus mediate greater gene silencing. To test this hypothesis, we prepared siRNA-loaded lipidoid nanoparticles of the exact same composition but with mean particle sizes ranging from 150 to 50 nm, which were created by extruding through membranes with different-sized pores. We used the standard composition of 98N<sub>12</sub>-5(1):cholesterol:mPEG<sub>2000</sub>-C14 = 42:48:10 (mol:mol:mol) with total lipid:siRNA = 7.5:1 (wt:wt). With this composition, we were unable to make stable liposomes with a mean diameter of <50 nm. The formulations were administered to mice at a dose

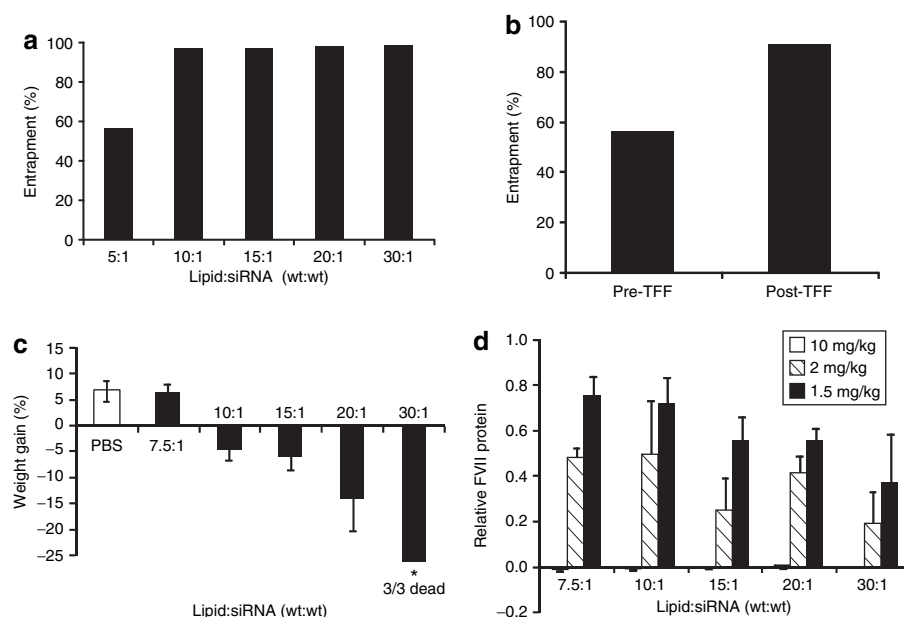


**Figure 2** Maximization of siRNA loading into 98N<sub>12</sub>-5(1)-based formulation. **(a)** siRNA entrapment at various initial lipid:siRNA (wt:wt) ratios. **(b)** Removal of nonentrapped siRNA from a formulation with initial lipid:siRNA ratio of 5:1 using tangential flow filtration (TFF) (100,000 molecular weight cutoff). Entrapment was measured before and after TFF with five volumes of buffer exchange. **(c,d)** C57BL/6 mice ( $n = 3$ ) received a single intravenous dose of 1.5, 2, or 10 mg/kg of Factor VII targeting siRNA formulated at different lipid:siRNA ratios. Control animals received saline injections. **(c)** Weight gain 48 hours postadministration for 10 mg/kg groups shown. **(d)** Serum Factor VII protein levels measured 48 hours postadministration. Data points represent group mean  $\pm$  SD. PBS, phosphate-buffered saline; siRNA, small interfering RNA.

of 3 mg/kg, and silencing of Factor VII was measured at 48 hours postadministration. Consistent with our hypothesis, we found that *in vivo* efficacy increased as mean particle size decreased (Figure 3c).

### Physical properties of LNP01

The final optimized formulation, which we termed “LNP01,” had a lipid composition of 98N<sub>12</sub>-5(1):cholesterol:PEG-lipid = 42:48:10 (mol:mol:mol), total lipid:siRNA = ~7.5:1 (wt:wt), C14 alkyl chain length on the PEG lipid, and a mean particle size of roughly 50–60 nm. Having established LNP01, we characterized some of its important physical properties. The volume-averaged particle size

distribution of LNP01 was determined by dynamic light-scattering measurements (Figure 4a). In addition, the formulation, which has maximally loaded siRNA, was found to have nearly neutral surface charge (+2–4 mV) as determined by zeta potential measurements (Figure 4b). Another critical physical property of a formulation designed for systemic nucleic acid delivery is the ability to protect the payload from nuclease degradation. The LNP01 formulation dramatically increases the nuclease resistance of a minimally chemically modified siRNA, increasing the  $t_{1/2}$  in serum from ~15 minutes to >24 hours (Figure 4c). This enhanced stability is likely a consequence of the entrapment of the siRNA, which limits its accessibility to serum nucleases. Finally, another parameter critical to the pharmaceutical

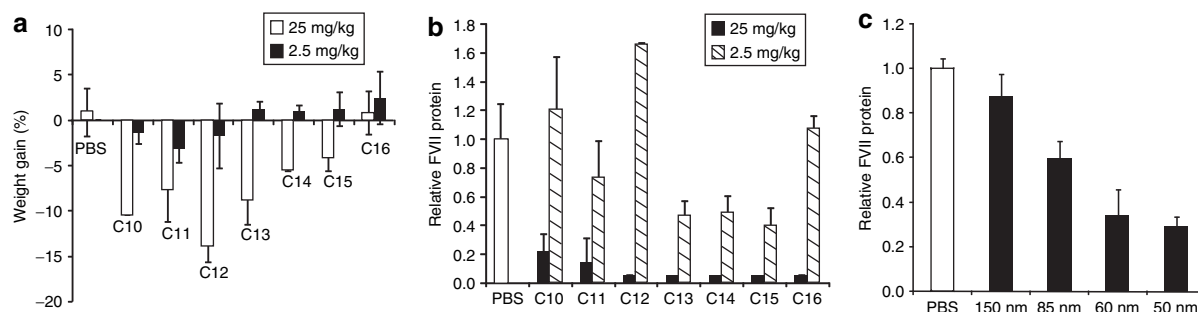


**Figure 3** Impact of PEG lipid alkyl chain length and particle size on *in vivo* activity. (a,b) C57BL/6 mice ( $n = 3$ ) received a single intravenous dose of either 2.5 or 20 mg/kg of Factor VII targeting siRNA formulated with PEG-lipids with different alkyl chain lengths (C10–C16). Control animals received saline injections. (a) Weight gain and (b) serum Factor VII protein levels 48 hours postadministration shown. (c) C57BL/6 mice ( $n = 3$ ) received a single intravenous dose of 3 mg/kg of Factor VII targeting siRNA formulated in lipidoid nanoparticles with different mean particle sizes. Control animals received saline injections. Serum Factor VII protein levels were measured 48 hours postadministration. Data points represent group mean  $\pm$  SD. PBS, phosphate-buffered saline; PEG, poly(ethylene glycol); siRNA, small interfering RNA.

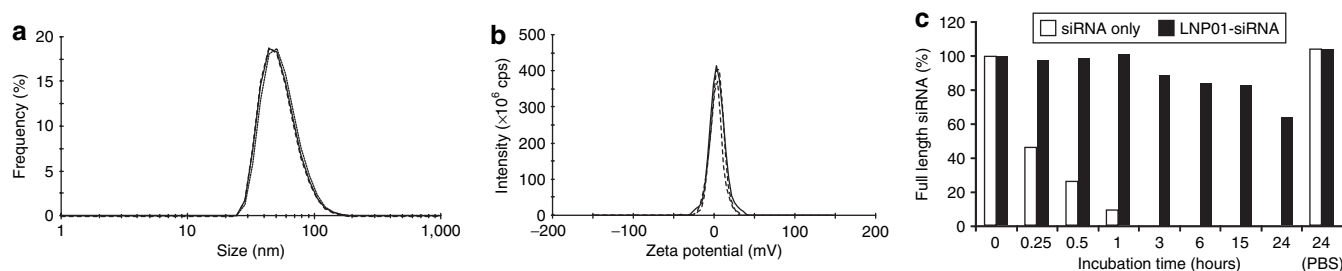


**Figure 4** Key physical attributes of LNP01. (a) Volume-averaged particle size distribution by dynamic light scattering. Data shown as an overlay of three independent measurements. (b) Zeta potential measurement in  $0.1\times$  PBS. Data shown as an overlay of three independent measurements. (c) Serum stability of unformulated and LNP01-formulated siRNA. Samples were incubated in human serum at 37°C for various times, and integrity of siRNA was measured using high-performance liquid chromatography. PBS, phosphate-buffered saline; siRNA, small interfering RNA.

**Table 1** Particle size distribution and small interfering RNA entrapment following storage

| Time (days) | 4°C           |            |                | 25°C          |            |                | 37°C          |            |                |
|-------------|---------------|------------|----------------|---------------|------------|----------------|---------------|------------|----------------|
|             | Diameter (nm) | Width (nm) | Entrapment (%) | Diameter (nm) | Width (nm) | Entrapment (%) | Diameter (nm) | Width (nm) | Entrapment (%) |
| 0           | 61            | 20         | 97             |               |            |                |               |            |                |
| 1           | 60            | 20         | 98             | 59            | 19         | 98             | 61            | 20         | 97             |
| 6           | 61            | 19         | 97             | 59            | 21         | 96             | 59            | 20         | 96             |
| 10          | 61            | 19         | 97             | 61            | 20         | 97             | 60            | 20         | 98             |
| 17          | 61            | 20         | 96             | 60            | 20         | 97             | 61            | 20         | 95             |
| 37          | 62            | 21         | 98             | 63            | 19         | 98             | 59            | 21         | 99             |
| 59          | 58            | 21         | 98             | 57            | 21         | 98             | 59            | 20         | 98             |
| 80          | 61            | 19         | 98             | 58            | 21         | 98             | 60            | 20         | 98             |
| 115         | 66            | 20         | 97             | 63            | 23         | 96             | 57            | 10         | 97             |
| 164         | 66            | 19         | 97             | 61            | 24         | 96             | 66            | 21         | 97             |

viability of a formulation is its stability during storage conditions. We typically store the LNP01 formulation in liquid solution under refrigerated conditions (2–8°C). We explored the physical stability of the formulation by storing LNP01-formulated siRNA at 4, 25, and 37°C for up to 5 months with regular sampling for measurements of particle size distribution and siRNA entrapment. Remarkably, over the entire duration of the study, we did not detect any evidence of aggregation or decreased entrapment of siRNA, even at elevated storage temperatures (Table 1). Furthermore, we have recently tested the *in vivo* activity of a formulation stored for 20 months at 4°C and found no change in efficacy (data not shown).

### Pharmacokinetics and biodistribution of LNP01

We investigated the pharmacokinetics and biodistribution of LNP01 administered to rats via single intravenous infusion (30-minute duration). LNP01 particles were labeled with <sup>3</sup>H-cholesteryl hexadecyl ether, and radioactivity in plasma and

tissues was measured by liquid scintillation spectroscopy. Animals were dosed at 3 mg/kg siRNA, which corresponded to a dose of 0.0020 mg/kg of <sup>3</sup>H-cholesteryl hexadecyl ether. The mean concentrations of plasma radioactivity are displayed in Table 2. Interestingly, LNP01 redistributes from the plasma into tissues remarkably quickly. The plasma  $t_{max}$  occurs at 1 hour, the first time point collected, and 30 minutes after the end of infusion. Furthermore, the 2.187 ng Eq/ml level at  $t_{max}$  corresponds to <4% of the injected dose. The tissue distribution and pharmacokinetics are displayed in Table 3. The data clearly indicate that the administered particles rapidly distribute primarily to liver. In fact, more than 90% of the administered dose is found in liver at the 1-hour time point, and the liver and spleen collectively account for more than 95% of the administered dose. In stark contrast to many cationic lipid formulations that accumulate in lung, only ~0.5% of LNP01 can be found in lung at 1 hour.

### Repeat administration of LNP01

The ability to maintain activity upon repeat administration is a critical property of a viable therapeutic. Sensitization can be a major issue limiting the effectiveness of biotherapeutics dosed repeatedly, either by stimulation of the innate immune response or by establishment of an adaptive immune response. Here, we show that LNP01 can be administered repeatedly with equal *in vivo* efficacy over extended time periods (Figure 5). To assess comparative efficacy, the repeated doses were administered after target protein levels had returned to baseline. Silencing with LNP01 has previously been shown to persist for >3 weeks after a single-bolus intravenous injection in rats and nonhuman primates.<sup>31</sup> This timescale is sufficiently long to allow for the establishment of a potential adaptive immune response. Mice were dosed with LNP01-formulated siRNA

**Table 2 Plasma pharmacokinetics of systemically-administered LNP01 (<sup>3</sup>H-labeled) in rats**

| Time point (hours) | Radioactivity Conc. (ng Eq/ml) | Percent of dose* |
|--------------------|--------------------------------|------------------|
| 1                  | 2.187 ± 0.153                  | 3.499 ± 0.245    |
| 3                  | 1.721 ± 0.404                  | 2.754 ± 0.646    |
| 5                  | 1.342 ± 0.360                  | 2.147 ± 0.576    |
| 7                  | 1.427 ± 0.268                  | 2.283 ± 0.429    |
| 24                 | 0.415 ± 0.105                  | 0.664 ± 0.168    |
| 96                 | 0.141 ± 0.009                  | 0.226 ± 0.014    |
| 168                | 0.096 ± 0.028                  | 0.154 ± 0.045    |

Conc., concentration.

\*Based on estimated plasma volume of 32 ml/kg.

**Table 3 Tissue biodistribution and pharmacokinetics of systemically-administered LNP01 (<sup>3</sup>H-labeled) in rats**

| Sample                   | Percent of dose |               |              |              |               |              |              |
|--------------------------|-----------------|---------------|--------------|--------------|---------------|--------------|--------------|
|                          | 1 hour          | 3 hours       | 5 hours      | 7 hours      | 24 hours      | 96 hours     | 168 hours    |
| Adrenal glands           | 0.14 ± 0.04     | 0.17 ± 0.08   | 0.16 ± 0.03  | 0.20 ± 0.04  | 0.18 ± 0.03   | 0.18 ± 0.02  | 0.21 ± 0.05  |
| Brain                    | 0.01 ± 0.00     | 0.01 ± 0.00   | 0.01 ± 0.00  | 0.01 ± 0.00  | 0.01 ± 0.00   | 0.01 ± 0.00  | 0.01 ± 0.00  |
| Carcass                  |                 |               |              |              |               |              | 5.53 ± 0.41  |
| Heart                    | 0.14 ± 0.06     | 0.04 ± 0.02   | 0.05 ± 0.01  | 0.05 ± 0.00  | 0.05 ± 0.01   | 0.04 ± 0.00  | 0.03 ± 0.01  |
| Kidneys                  | 0.56 ± 0.12     | 0.27 ± 0.07   | 0.20 ± 0.05  | 0.26 ± 0.01  | 0.25 ± 0.01   | 0.21 ± 0.02  | 0.17 ± 0.02  |
| Liver                    | 90.78 ± 5.86    | 86.87 ± 21.28 | 87.85 ± 6.80 | 91.85 ± 7.06 | 64.43 ± 32.29 | 49.06 ± 8.99 | 37.48 ± 4.31 |
| Lungs                    | 0.52 ± 0.08     | 0.23 ± 0.06   | 0.27 ± 0.04  | 0.25 ± 0.02  | 0.26 ± 0.04   | 0.24 ± 0.02  | 0.17 ± 0.01  |
| Lymph nodes (mesenteric) | 0.01 ± 0.00     | 0.01 ± 0.00   | 0.01 ± 0.00  | 0.02 ± 0.01  | 0.02 ± 0.01   | 0.02 ± 0.01  | 0.02 ± 0.01  |
| Pancreas                 | 0.06 ± 0.02     | 0.03 ± 0.01   | 0.04 ± 0.02  | 0.04 ± 0.01  | 0.05 ± 0.03   | 0.05 ± 0.05  | 0.04 ± 0.01  |
| Spleen                   | 5.20 ± 1.26     | 4.94 ± 1.14   | 5.53 ± 0.82  | 4.82 ± 1.00  | 5.97 ± 0.57   | 5.43 ± 0.49  | 4.23 ± 0.63  |
| Testes                   | 0.03 ± 0.01     | 0.04 ± 0.01   | 0.04 ± 0.00  | 0.05 ± 0.00  | 0.07 ± 0.01   | 0.08 ± 0.00  | 0.08 ± 0.01  |
| Thymus                   | 0.01 ± 0.00     | 0.01 ± 0.00   | 0.01 ± 0.00  | 0.01 ± 0.00  | 0.01 ± 0.00   | 0.01 ± 0.00  | 0.01 ± 0.00  |
| Small intestine          | 0.37 ± 0.03     | 0.35 ± 0.13   | 0.32 ± 0.06  | 0.38 ± 0.07  | 0.85 ± 0.07   | 0.55 ± 0.09  | 0.41 ± 0.08  |
| Small intestine contents | 0.45 ± 0.04     | 0.89 ± 0.24   | 0.58 ± 0.08  | 0.62 ± 0.10  | 3.89 ± 0.89   | 1.23 ± 0.17  | 0.59 ± 0.22  |
| Large intestine          | 0.12 ± 0.00     | 0.10 ± 0.03   | 0.11 ± 0.02  | 0.13 ± 0.02  | 0.23 ± 0.04   | 0.14 ± 0.01  | 0.11 ± 0.01  |
| Large intestine contents | 0.00 ± 0.00     | 0.00 ± 0.00   | 0.62 ± 0.05  | 0.84 ± 0.05  | 9.24 ± 3.18   | 3.34 ± 0.87  | 0.98 ± 0.19  |
| Stomach                  | 0.07 ± 0.02     | 0.03 ± 0.01   | 0.05 ± 0.04  | 0.04 ± 0.01  | 0.07 ± 0.04   | 0.04 ± 0.01  | 0.03 ± 0.00  |
| Stomach contents         | 0.00 ± 0.01     | 0.00 ± 0.01   | 0.00 ± 0.00  | 0.00 ± 0.00  | 0.06 ± 0.09   | 0.01 ± 0.01  | 0.05 ± 0.05  |



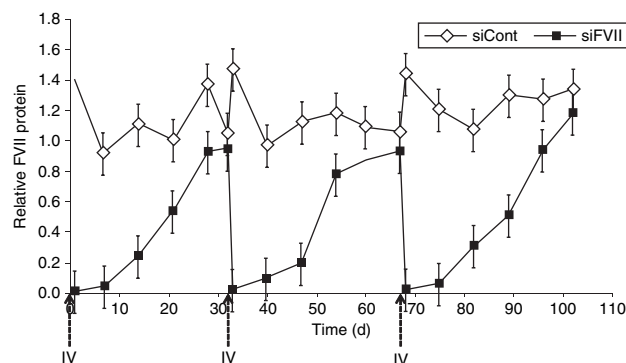


**Figure 5 Activity is maintained upon repeat administration of LNP01.** C57BL/6 mice ( $n = 5$ ) received a bolus intravenous (IV) injection of either saline, LNP01-formulated control siRNA (siCont) at 5 mg/kg, or LNP01-formulated Factor VII targeting siRNA (siFVII) at 5 mg/kg. Serum samples were collected at various time points and Factor VII protein levels were determined in the samples. After recovery of Factor VII levels to baseline values, animals were redosed on the indicated days. Data were collected for three treatment cycles. Data are displayed as relative to saline-treated control values for each time point and represent mean values  $\pm$  SD. siRNA, small interfering RNA.

targeting Factor VII. Serum samples were collected at various time points postadministration, and Factor VII levels were quantified relative to levels of saline control-treated animals. Upon recovery of serum Factor VII levels to baseline, corresponding to approximately 1 month, animals were redosed. Data were collected for a total of three cycles. The silencing profiles were virtually indistinguishable, with no observable change in the maximal level of silencing or kinetics of recovery to baseline levels. Furthermore, the treatment did not result in any observable negative effects, and mice in all groups gained weight normally during the study.

## DISCUSSION

The advancement of the promising field of RNA interference therapeutics requires the development of safe and effective siRNA delivery systems. Formulations based on lipid and lipid-like materials have been studied and show great promise as siRNA delivery agents. Here, we describe the development of a lipidoid-based formulation for the systemic delivery of siRNA to hepatocytes *in vivo*. Although we were guided by certain theoretical considerations (e.g., small particle size, minimal charge, and maximal siRNA loading), we generally employed an empirical approach to maximize efficacy and minimize toxicity *in vivo*.

In a prior study, we described the synthesis and screening of a combinatorial library of lipid-like compounds to identify novel materials for the delivery of siRNA.<sup>31</sup> One of the lead compounds that emerged from that library, 98N<sub>12</sub>-5(1), formed the basis for the formulation described in this work. The novel compound 98N<sub>12</sub>-5(1) was combined with cholesterol and a PEG lipid to form nanoparticles capable of encapsulating siRNA. The molar ratios of 98N<sub>12</sub>-5(1), cholesterol, and PEG lipid were varied to determine the parameter space that led to the formation of stable, siRNA-loaded particles under the formulation conditions we employed. Admittedly, different formulation conditions or processes may lead to different compositions that are available for formulation and testing. Various compositions were tested for *in vivo* efficacy and the optimal composition of 98N<sub>12</sub>-5(1):cholesterol:PEG-lipid = 42:48:10 (mol:mol:mol) was selected.

In this study, we extended our prior work by elucidating the impact of various formulation parameters on *in vivo* pharmacodynamics. It is known that cationic liposomes and lipid formulations can be associated with toxicity *in vivo*; therefore, we sought to ameliorate this effect by limiting the surface charge and by minimizing the total amount of administered lipids. We hypothesized that maximizing siRNA loading would lead to a better-tolerated formulation, but we were unsure how the ratio of lipid to siRNA would affect *in vivo* efficacy. To address this question, we prepared and tested formulations with different initial lipid:siRNA weight ratios (Figure 2). We first measured entrapment efficiency to determine the point of maximal siRNA loading, which occurred at a lipid:siRNA ratio of  $\sim$ 7.5:1 (wt:wt). *In vivo* testing demonstrated that reducing the lipid:siRNA ratio had only a slightly negative effect on efficacy, while having a very significant positive effect on tolerability. Thus, we found that maximizing siRNA loading resulted in an optimized formulation. We then turned our attention to optimizing the alkyl chain length of the PEG lipid. We expected the alkyl chain length to affect the rate of PEG lipid disassociation, and thus, particle unshielding. The rate of particle unshielding may in turn affect *in vivo* pharmacodynamics. We synthesized PEG lipids with various anchor lengths ranging from C10 to C16. We found that increasing the anchor length led to improved tolerability, but that efficacy was optimized for anchor lengths of C13–C15. Therefore, we concluded that C14- and C15-based PEG-lipids yielded formulations with the optimal balance of efficacy and tolerability (Figure 3a,b). However, due to the relative availability of synthetic starting materials, we ultimately selected the PEG–C14 lipid. Finally, we verified our assumption that smaller particles would have more efficient access to hepatocytes via the fenestrated endothelium of the liver. We prepared formulations of identical composition, but with particle sizes ranging from 50 to 150 nm. Consistent with our hypothesis, we observed a clear trend of increasing *in vivo* efficacy with decreasing particle size (Figure 3c).

The final optimized formulation, “LNP01,” had a lipid composition of 98N<sub>12</sub>-5(1):cholesterol:PEG lipid = 42:48:10 (mol:mol:mol), total lipid:siRNA =  $\sim$ 7.5:1 (wt:wt), C14 alkyl chain length on the PEG lipid, and a particle size of roughly 50–60 nm. In this work, we report key physical properties of LNP01, such as the particle size distribution of LNP01 (Figure 4a) and its near-neutral surface charge (Figure 4b). Consistent with the stable entrapment of siRNA, we demonstrated that formulation in LNP01 imparts nuclease stability to an inherently unstable siRNA, increasing  $t_{1/2}$  from 15 minutes to more than 24 hours (Figure 4c). This characteristic obviates the need to extensively modify the siRNA payload to achieve efficacy *in vivo*. Many nucleic acid delivery systems (e.g., lipoplexes and polyplexes) are unstable and aggregate over time. As stability is a critical parameter that affects the suitability of a formulation for its pharmaceutical use, we investigated the storage stability of LNP01. We were encouraged to find that the formulation was stable for many months, even under conditions of elevated storage temperature (Table 1). We also examined the pharmacokinetics and tissue biodistribution of LNP01 in rats. We found that LNP01 distributes from the plasma remarkably quickly, with <4% of the injected dose remaining in plasma at the 1-hour time point (Table 2). The tissue biodistribution data

clearly indicate that the material distributes primarily to liver, with more than 90% of the injected dose found in the liver at 1 hour (Table 3). It is interesting to note that although the formulation was not directly optimized for specific liver delivery, this property emerged as a consequence of our efforts to develop and optimize LNP01 for highly effective hepatic gene silencing with minimal toxicity *in vivo*. Finally, another key attribute of a viable therapeutic is the ability to be repeatedly administered *in vivo*. Sensitization, by stimulation of either the innate or adaptive immune responses, can be a concern for biotherapeutics that are administered repeatedly. We dosed animals multiple times with LNP01, allowing 1 month each time for recovery of target protein levels to baseline prior to the next dose. We observed no change in silencing activity or silencing kinetics upon repeat administration, suggesting that the formulation may be made suitable for applications requiring repeat dosing (Figure 5). However, it is clear that more work is required to establish efficacy and tolerability for longer-term, chronic applications.

In summary, we have described the development of a novel formulation for the systemic delivery of siRNA to hepatocytes. We identified key parameters affecting the pharmacodynamics of the formulation, and we optimized these parameters to yield an appropriate balance between efficacy and tolerability *in vivo*. This new formulation, termed LNP01, has been used successfully to silence multiple (>10) genes in multiple species (mouse, rat, hamster, and monkey), both in our labs and the labs of our collaborators. LNP01 has proven a useful tool for *in vivo* target validation and may also hold promise for therapeutic use.

## MATERIALS AND METHODS

**siRNAs.** All siRNAs were synthesized by Alnylam and were characterized by ESMS and anion-exchange HPLC. The sequences for the sense and antisense strands of siRNAs are as follows:

siFVII sense: 5'-GGAucAucucAAGucuuAcT\*T-3', antisense: 5'-GuAAGAcuuGAGAuGAuccT\*T-3'.

siCont sense: 5'-cuuAcGcuGAGuAcuucGAT\*T-3', antisense: 5'-UCGAAGuACuAcGCGuAAGT\*T-3'.

2'-O-Me modified nucleotides are in lower case, 2'-Fluoro-modified nucleotides are in bold lower case, and phosphorothioate linkages are represented by asterisks. siRNAs were generated by annealing equimolar amounts of complementary sense and antisense strands.

**Lipid synthesis.** The synthesis of 98N<sub>12</sub>-5(1) and mPEG<sub>2000</sub> lipids was done as previously described.<sup>31</sup>

**Lipid-siRNA Formulation.** Lipid-siRNA formulations comprised 98N<sub>12</sub>-5(1), cholesterol, PEG-lipid, and siRNA. Formulations were prepared as previously described.<sup>31</sup> Briefly, stock solutions of 98N<sub>12</sub>-5(1), mPEG<sub>2000</sub>-lipid, and cholesterol (Sigma-Aldrich, St Louis, MO) were prepared in ethanol and mixed to yield the desired molar ratios. Mixed lipids were added to 125 mmol/l sodium acetate buffer (pH 5.2) to yield a solution containing 35% ethanol, resulting in spontaneous formation of empty lipidoid nanoparticles. The resultant nanoparticles were extruded through a 0.08 µm membrane (Sterlitech, Kent, WA) using a LIPEX Extruder (Northern Lipids, Burnaby, British Columbia, Canada) to form particles 50–60 nm in length. To study the effect of particle size on activity, formulations of larger size were generated by first allowing the initial empty lipidoid nanoparticle mixture to incubate for ~24 hours at 4°C. Extrusion was then carried out using 0.4, 0.2, and 0.1 µm membranes

to yield formulations of larger size. siRNA in 50 mmol/l sodium acetate (pH 5.2) and 35% ethanol was added to the nanoparticles at the desired total lipid:siRNA ratios and incubated at 37°C for 30 minutes. Ethanol removal and buffer exchange of siRNA-containing lipidoid nanoparticles was achieved by dialysis against phosphate-buffered saline. Finally, the formulation was filtered through a 0.2 µm sterile filter. Particle size and zeta potential were determined using a Malvern Zetasizer NanoZS (Malvern, UK). siRNA content was determined by ultraviolet absorption at 260 nm, and siRNA entrapment efficiency was determined by the Quant-iT RiboGreen RNA assay (Invitrogen, Carlsbad, CA).<sup>41</sup> Briefly, siRNA entrapment is determined by comparing the signal of the RNA binding dye RiboGreen in formulation samples in the absence and presence of the detergent Triton-X100. In the absence of detergent, signal comes from accessible (unentrapped) siRNA only. In the presence of detergent, signal comes from total siRNA.

**In vivo rodent Factor VII silencing experiments.** All procedures used in animal studies conducted at Alnylam were approved by the Institutional Animal Care and Use Committee and were consistent with local, state, and federal regulations, as applicable. C57BL/6 mice (Charles River Labs, Wilmington, MA) received either saline or siRNA in lipid formulations via tail vein injection at a volume of 0.01 ml/g. Serum levels of Factor VII protein were determined in samples collected by retroorbital bleed using an activity-based chromogenic assay (Biophen FVII; Aniara, Mason, OH).

**Pharmacokinetics and biodistribution experiments.** All procedures were conducted by a certified contract research organization using protocols consistent with local, state, and federal regulations as applicable and approved by the Institutional Animal Care and Use Committee. Male Sprague-Dawley rats were administered a single intravenous infusion dose, via an Abbot cath placed in the lateral tail vein (30-minute duration), of 3 mg/kg siRNA formulated in radiolabeled LNP01 (<sup>3</sup>H-lipidoid nanoparticles). <sup>3</sup>H-cholesteryl hexadecyl ether was incorporated in the particles during formulation such that animals received 0.0020 mg/kg of <sup>3</sup>H-cholesteryl hexadecyl ether. Blood and tissue samples were collected at 1, 3, 5, 7, 24, 96, and 168 hours poststart of dose from three animals/time point (except 168-hour time point, where *n* = 5). The concentration of radioactivity in plasma and tissues was determined by liquid scintillation counting.

## ACKNOWLEDGMENTS

We acknowledge NIH EB00244 and a grant from Alnylam. We also thank Maryellen Livingston for assistance with manuscript preparation.

## REFERENCES

- Dickins, RA, McJunkin, K, Hernando, E, Premisrur, PK, Krizhanovsky, V, Burgess, DJ *et al.* (2007). Tissue-specific and reversible RNA interference in transgenic mice. *Nat Genet* **39**: 914–921.
- Soutschek, J, Akinc, A, Bramlage, B, Charisse, K, Constien, R, Donoghue, M *et al.* (2004). Therapeutic silencing of an endogenous gene by systemic administration of modified siRNAs. *Nature* **432**: 173–178.
- de Fougerolles, A, Vornlocher, H-P, Maraganore, J and Lieberman, J (2007). Interfering with disease: a progress report on siRNA-based therapeutics. *Nat Rev Drug Discov* **6**: 443–453.
- Novina, CD and Sharp, PA (2004). The RNAi revolution. *Nature* **430**: 161–164.
- Check, E (2005). Gene therapy put on hold as third child develops cancer. *Nature* **433**: 561.
- Boyce, N (2001). Trial halted after gene shows up in semen. *Nature* **414**: 677.
- Zhang, S, Zhao, B, Jiang, H, Wang, B and Ma, B (2007). Cationic lipids and polymers mediated vectors for delivery of siRNA. *J Control Release* **123**: 1–10.
- Wagner, E, Kircheis, R and Walker, GF (2004). Targeted nucleic acid delivery into tumors: new avenues for cancer therapy. *Biomed Pharmacother* **58**: 152–161.
- Liu, F and Huang, L (2002). Development of non-viral vectors for systemic gene delivery. *J Control Release* **78**: 259–266.
- Li, W and Szoka, F (2007). Lipid-based nanoparticles for nucleic acid delivery. *Pharm Res* **24**: 438–449.
- Panyam, J and Labhasetwar, V (2003). Biodegradable nanoparticles for drug and gene delivery to cells and tissue. *Adv Drug Deliv Rev* **55**: 329–347.
- Zimmermann, TS, Lee, ACH, Akinc, A, Bramlage, B, Bumcrot, D, Fedoruk, MN *et al.* (2006). RNAi-mediated gene silencing in non-human primates. *Nature* **441**: 111–114.
- Song, E, Lee, S-K, Wang, J, Ince, N, Ouyang, N, Min, J *et al.* (2003). RNA interference targeting Fas protects mice from fulminant hepatitis. *Nat Med* **9**: 347–351.

14. Song, E, Zhu, P, Lee, S-K, Chowdhury, D, Kussman, S, Dykxhoorn, DM *et al.* (2005). Antibody mediated *in vivo* delivery of small interfering RNAs via cell-surface receptors. *Nat Biotech* **23**: 709–717.
15. Morrissey, DV, Lockridge, JA, Shaw, L, Blanchard, K, Jensen, K, Breen, W *et al.* (2005). Potent and persistent *in vivo* anti-HBV activity of chemically modified siRNAs. *Nat Biotech* **23**: 1002–1007.
16. Kim, SI, Shin, D, Choi, TH, Lee, JC, Cheon, G-J, Kim, K-Y *et al.* (2007). Systemic and specific delivery of small interfering RNAs to the liver mediated by apolipoprotein A-I. *Mol Ther* **15**: 1145–1152.
17. Baigude, H, McCarroll, J, Yang, CS, Swain, PM and Rana, TM (2007). Design and creation of new nanomaterials for therapeutic RNAi. *ACS Chem Biol* **2**: 237–241.
18. Santel, A, Aleku, M, Keil, O, Endruschat, J, Esche, V, Fisch, G *et al.* (2006). A novel siRNA-lipoplex technology for RNA interference in the mouse vascular endothelium. *Gene Ther* **13**: 1222–1234.
19. Hu-Lieskovan, S, Heidel, JD, Bartlett, DW, Davis, ME and Triche, TJ (2005). Sequence-specific knockdown of EWS-FLI1 by targeted, nonviral delivery of small interfering RNA inhibits tumor growth in a murine model of metastatic Ewing's sarcoma. *Cancer Res* **65**: 8984–8992.
20. Takeshita, F, Minakuchi, Y, Nagahara, S, Honma, K, Sasaki, H, Hirai, K *et al.* (2005). Efficient delivery of small interfering RNA to bone-metastatic tumors by using atelocollagen *in vivo*. *Proc Natl Acad Sci USA* **102**: 12177–12182.
21. Rozema, DB, Lewis, DL, Wakefield, DH, Wong, SC, Klein, JJ, Roesch, PL *et al.* (2007). Dynamic PolyConjugates for targeted *in vivo* delivery of siRNA to hepatocytes. *Proc Natl Acad Sci USA* **104**: 12982–12987.
22. Peer, D, Park, EJ, Morishita, Y, Carman, CV and Shimaoka, M (2008). Systemic leukocyte-directed siRNA delivery revealing Cyclin D1 as an anti-inflammatory target. *Science* **319**: 627–630.
23. Wolfrum, C, Shi, S, Jayaprakash, KN, Jayaraman, M, Wang, G, Pandey, RK *et al.* (2007). Mechanisms and optimization of *in vivo* delivery of lipophilic siRNAs. *Nat Biotech* **25**: 1149–1157.
24. de Fougerolles, A (2008). Delivery vehicles for small interfering RNA *in vivo*. *Human Gene Ther* **19**: 125–132.
25. Wisse, E, Jacobs, F, Topal, B, Frederik, P and De Geest, B (2008). The size of endothelial fenestrae in human liver sinusoids: implications for hepatocyte-directed gene transfer. *Gene Ther* **15**: 1193–1199.
26. Medina-Kauwe, LK, Xie, J and Hamm-Alvarez, S (2005). Intracellular trafficking of nonviral vectors. *Gene Ther* **12**: 1734–1751.
27. Wattiaux, R, Laurent, N, Wattiaux-De Coninck, S and Jadot, M (2000). Endosomes, lysosomes: their implication in gene transfer. *Adv Drug Deliv Rev* **41**: 201–208.
28. Mui, B, Ahkong, QF, Chow, L and Hope, MJ (2000). Membrane perturbation and the mechanism of lipid-mediated transfer of DNA into cells. *Biochim Biophys Acta* **1467**: 281–292.
29. Sonawane, ND, Szoka, FC and Verkman, AS (2003). Chloride accumulation and swelling in endosomes enhances DNA transfer by polyamine-DNA polyplexes. *J Biol Chem* **278**: 44826–44831.
30. Satija, J, Gupta, U and Jain, NK (2007). Pharmaceutical and biomedical potential of surface engineered dendrimers. *Crit Rev Ther Drug Carrier Syst* **24**: 257–306.
31. Akinc, A, Zumbuehl, A, Goldberg, M, Leshchiner, E, Busini, V, Bacallado, S *et al.* (2008). A combinatorial library of lipid-like materials for delivery of RNAi therapeutics. *Nat Biotech* **26**: 561–569.
32. Abraham, SA, Waterhouse, DN, Mayer, LD, Cullis, PR, Madden, TD and Bally, MB (2005). The liposomal formulation of doxorubicin. *Methods Enzymol* **391**: 71–97.
33. Fenske, DB and Cullis, PR (2008). Liposomal nanomedicines. *Expert Opin Drug Deliv* **5**: 25–44.
34. Maurer, N, Mori, A, Palmer, L, Monck, MA, Mok, KW, Mui, B *et al.* (1999). Lipid-based systems for the intracellular delivery of genetic drugs. *Mol Membr Biol* **16**: 129–140.
35. Judge, AD, Sood, V, Shaw, JR, Fang, D, McClintock, K and MacLachlan, I (2005). Sequence-dependent stimulation of the mammalian innate immune response by synthetic siRNA. *Nat Biotechnol* **23**: 457–462.
36. Semple, SC, Klimuk, SK, Harasym, TO, Dos Santos, N, Ansell, SM, Wong, KF *et al.* (2001). Efficient encapsulation of antisense oligonucleotides in lipid vesicles using ionizable aminolipids: formation of novel small multilamellar vesicle structures. *Biochim Biophys Acta* **1510**: 152–166.
37. Wheeler, JJ, Palmer, L, Ossanlou, M, MacLachlan, I, Graham, RW, Zhang, YP *et al.* (1999). Stabilized plasmid-lipid particles: construction and characterization. *Gene Ther* **6**: 271–281.
38. Immordino, ML, Dosio, F and Cattel, L (2006). Stealth liposomes: review of the basic science, rationale, and clinical applications, existing and potential. *Int J Nanomedicine* **1**: 297–315.
39. Adlakha-Hutcheon, G, Bally, MB, Shew, CR and Madden, TD (1999). Controlled destabilization of a liposomal drug delivery system enhances mitoxantrone antitumor activity. *Nature Biotech* **17**: 775–779.
40. Webb, MS, Saxon, D, Wong, FM, Lim, HJ, Wang, Z, Bally, MB *et al.* (1998). Comparison of different hydrophobic anchors conjugated to poly(ethylene glycol): effects on the pharmacokinetics of liposomal vincristine. *Biochim Biophys Acta* **1372**: 272–282.
41. Heyes, J, Palmer, L, Bremner, K and MacLachlan, I (2005). Cationic lipid saturation influences intracellular delivery of encapsulated nucleic acids. *J Control Release* **107**: 276–287.